A&A 564, A76 (2014)
DOI: 10.1051/0004-6361/201323180

Astronomy & Astrophysics

The narrow and moving HeII lines in nova KT Eridani

U. Munari[1], E. Mason[2], and P. Valisa[3]

[1] INAF Osservatorio Astronomico di Padova, 36012 Asiago (VI), Italy
e-mail: ulisse.munari@oapd.inaf.it
[2] INAF Osservatorio Astronomico di Trieste, 34143 Trieste, Italy
[3] ANS Collaboration, c/o Osservatorio Astronomico, 36012 Asiago (VI), Italy

Received 3 December 2013 / Accepted 28 February 2014

ABSTRACT

We present outburst and quiescence spectra of the classical nova KT Eri and discuss the appearance of a sharp HeII 4686 Å emission line, whose origin is a matter of discussion for those novae that showed a similar component. We suggest that the sharp HeII line, when it first appeared toward the end of the outburst optically thick phase, comes from the wrist of the dumbbell structure characterizing the ejecta. When the ejecta turned optically thin, the already sharp HeII line became two times narrower and originated from the exposed central binary. During the optically thin phase, the HeII line displayed a large change in radial velocity that had no counterpart in the Balmer lines (both their narrow cores and the broad pedestals). The large variability in radial velocity of the HeII line continued well into quiescence, and it remains the strongest emission line observed over the whole optical range.

Key words. novae, cataclysmic variables – stars: individual: KT Eridani

1. Introduction

Nova Eri 2009, later named KT Eri, was discovered by K. Itagaki on 2009 November 25.5 UT (see CBET 2050), well past its optical maximum. Using data obtained by Solar Mass Ejection Imager (SMEI) on board the *Coriolis* satellite, Hounsell et al. (2011) were able to reconstruct the pre-discovery outburst light curve, which highlights a rapid rise in magnitude after the first detection on 2009 November 13.12 UT, a sharp maximum reached on 2009 November 14.67 UT, after which the nova immediately entered the rapid decline characterized by $t_2 = 6.6$ days. Preliminary reports on the early spectroscopic and photometric evolution were provided by Ragan et al. (2009), Rudy et al. (2009), Bode et al. (2010), Imamura & Tanabe (2012), and Hung et al. (2012). Radio observations were obtained by O'Brien et al. (2010) and X-ray observations by Bode et al. (2010), Beardmore et al. (2010), and Ness et al. (2010). Raj et al. (2013) discussed early infrared photometric and spectroscopic evolution, while the line profiles and their temporal evolution were modeled in detail by Ribeiro et al. (2013). Jurdana-Šepić et al. (2012) searched the Harvard plate archive and measured the progenitor of the nova on 1012 plates dating from 1888 to 1962. No previous outburst was found. The photometric evolution of KT Eri after it returned to quiescence and its persistent $P = 752$ day periodicity have been discussed by Munari & Dallaporta (2014).

Here we present KT Eri spectra taken from outburst maximum to subsequent quiescence and focus on the appearance and evolution of a narrow HeII 4686 Å emission line. Sharp emission lines superimposed to much broader emission components, have been observed in a few other recent novae: YY Dor, nova LMC 2009, U Sco, DE Cir, and V2672 Oph (see, e.g., the Stony Brooks SMART Atlas[1]). Complex line profiles have always been modeled with axisymmetric ejecta geometries consisting of bipolar lobes, polar caps, and equatorial rings (starting with Payne-Gaposchkin in 1957). Using a similar approach, the sharp and strong narrow emission in V2672 Oph could be successfully modeled as coming from an equatorial ring whereas the broader pedestal originates from polar cups (Munari et al. 2011). However, because of their sharpness, profile, and width it has been also suggested that the narrow components in the above systems might arise from the accretion disk of the underlying binary (Walter & Battisti 2011, but see also Mason & Walter 2013), once the ejecta becomes sufficiently transparent. In the case of U Sco, the observation of radial velocity motion of the narrow HeII emission has been interpreted as restored accretion shortly after the nova 2010 outburst (Mason et al. 2012). Whether a narrow emission component, and in particular the appearance of the sharp HeIIλ4686 line, always originates in the central binary and recovered accretion from the secondary star has to be established.

We believe KT Eri offers an interesting bridge between these two alternative views. We will show how when first seen in emission in the spectra of KT Eri, during the optically thick phase, the sharp HeII 4686 Å line was coming from the inner and slower regions of the ejecta, and how, at later times when the ejecta turned optically thin, the HeII line became two times sharper and variable in radial velocity, indicating it was coming directly from the central binary. Thus, the presence and the origin of sharp HeII emission lines seems to depend on the geometry of the ejecta, their viewing angle, and on the evolutionary phase of the nova.

2. Observations

Absolute spectroscopy of KT Eri was obtained during the outburst as part of the long-term ANS Collaboration monitoring of novae in eruption (see Munari et al. 2012). We used the Varese 0.61m telescope equipped with the mark.II Multi Mode

[1] http://www.astro.sunysb.edu/fwalter/SMARTS/NovaAtlas/atlas.html

Table 1. Logbook of our spectroscopic observations of KT Eri.

Date	UT	HJD (−2 450 000)	Δ*t* (days)	Res. pow.	disp (Å/pix)	Range (Å)	Expt (s)	Tel
2009 Dec. 01	20:54	5167.376	17.21	17,000		3950–8650	4 × 900	0.61 m
2009 Dec. 01	22:09	5167.428	17.26		2.12	3960–8610	2 × 300	0.61 m
2009 Dec. 05	20:22	5171.353	21.18		2.12	3700–8000	3 × 300	0.61 m
2009 Dec. 05	19:58	5171.337	21.17		2.12	3960–8500	3 × 300	0.61 m
2009 Dec. 09	20:10	5175.345	25.17	17,000		3950–8650	4 × 900	0.61 m
2009 Dec. 15	19:28	5181.316	31.15		2.12	3950–8600	2 × 300	0.61 m
2009 Dec. 17	21:17	5183.391	33.22		2.12	3950–8600	3 × 600	0.61 m
2009 Dec. 19	21:37	5185.405	35.23	11,000		3875–8630	5 × 900	0.61 m
2010 Jan. 06	18:18	5203.266	53.10		2.12	3950–8600	2 × 600	0.61 m
2010 Jan. 18	21:06	5215.382	65.21		2.12	3900–8550	3 × 600	0.61 m
2010 Jan. 24	18:43	5221.283	71.11		2.12	3800–8440	3 × 600	0.61 m
2010 Jan. 24	20:08	5221.342	71.17		0.71	5435–7035	4 × 900	0.61 m
2010 Jan. 24	21:45	5221.409	71.24		0.71	3930–5700	4 × 900	0.61 m
2010 Jan. 28	19:23	5225.310	75.14		2.12	3800–8445	4 × 900	0.61 m
2010 Feb. 02	19:22	5230.309	80.14		0.71	3800–5550	4 × 900	0.61 m
2010 Feb. 02	20:41	5230.364	80.19		0.71	5500–7090	4 × 900	0.61 m
2010 Feb. 06	20:27	5234.354	84.18		4.24	3730–8370	3 × 900	0.61 m
2010 Feb. 13	21:24	5241.393	91.22		4.24	3725–8360	7 × 900	0.61 m
2010 Feb. 20	19:48	5248.326	98.16		4.24	3750–8340	8 × 900	0.61 m
2010 Mar. 16	19:27	5272.309	122.14		4.24	3800–8315	2 × 900	0.61 m
2013 Jan. 05	21:36	6298.404	1148.23		2.31	3350–8050	3 × 1200	1.22 m
2013 Jan. 06	21:00	6299.379	1149.21		2.31	3350–8050	4 × 1800	1.22 m
2013 Jan. 26	19:59	6319.335	1169.16		2.31	3350–8050	3 × 1200	1.22 m
2013 Mar. 02	18:04	6354.252	1204.08		2.31	3350–8050	1 × 1500	1.22 m
2013 Mar. 04	18:12	6356.258	1206.09		2.31	3350–8050	1 × 1500	1.22 m
2013 Dec. 13	21:05	6640.379	1490.21		2.31	3400–7950	3 × 1200	1.22 m
2014 Feb. 09	19:31	6698.313	1548.14		2.31	3400–7950	6 × 1200	1.22 m
2014 Feb. 12	18:43	6701.280	1551.11		2.31	3400–7950	6 × 1200	1.22 m

Notes. Resolving power is listed for the Echelle high-resolution observations, dispersion for the medium- and low-resolution spectra. Δ*t* is the time past the optical maximum as fixed by SMEI observations (2009 November 14.67 UT or HJD = 2 455 150.17; Hounsell et al. 2011).

Table 2. Visibility and integrated absolute flux of HeII 4686 Å emission line in our spectra of KT Eri.

Date	HJD	HeII 4686 Å (erg cm^{-2} s^{-1})	Date	HJD	HeII 4686 Å (erg cm^{-2} s-1)
2009 Dec. 01	5167.376	no	2010 Feb. 02	5230.309	1.81E-12
2009 Dec. 01	5167.428	no	2010 Feb. 06	5234.354	1.59E-12
2009 Dec. 05	5171.353	no	2010 Feb. 13	5241.393	1.72E-12
2009 Dec. 05	5171.337	no	2010 Feb. 20	5248.326	1.64E-12
2009 Dec. 09	5175.345	no	2010 Mar. 16	5272.309	1.25E-12
2009 Dec. 15	5181.316	no	2013 Jan. 05	6298.404	2.72E-14
2009 Dec. 17	5183.391	no	2013 Jan. 06	6299.379	2.92E-14
2009 Dec. 19	5185.405	no	2013 Jan. 26	6319.335	4.84E-14
2010 Jan. 06	5203.266	7.24E-12	2013 Mar. 02	6354.252	3.25E-14
2010 Jan. 18	5215.382	1.95E-11	2013 Mar. 04	6356.258	3.99E-14
2010 Jan. 24	5221.283	3.71E-12	2013 Dec. 13	6640.379	3.38E-14
2010 Jan. 24	5221.409	4.32E-12	2014 Feb. 09	6698.313	4.36E-14
2010 Jan. 28	5225.310	2.24E-12	2014 Feb. 12	6701.280	4.50E-14

Spectrograph (Munari & Valisa 2014), that allows rapid switching between low-dispersion, medium-dispersion and Echelle high-resolution modes. A 2 arcsec wide slit, aligned along the parallactic angle was used in all observations. Echelle spectra were calibrated with a thorium lamp exposed before and after the science spectra, and similarly with a FeHeAr lamp for the medium- and low-dispersion spectra. Flux calibration was achieved via observation of the nearby spectrophotometric standard HR 1784 observed with the identical instrumental setup both immediately before and soon after the nova. All data reduction was carried out in IRAF, following standard extraction procedures involving correction for bias, dark, and flat and sky background subtraction.

Low-resolution absolute spectroscopy of KT Eri, after it returned to quiescence brightness long after the end of the outburst, was obtained with the Asiago 1.22 m telescope and B&C single dispersion spectrograph. Also in this case we adopted a 2 arcsec wide slit, aligned along the parallactic angle, the same spectrophotometric standard star and the same extraction/calibration procedures as for the observations obtained with the 0.61 m telescope during the outburst phase.

Table 1 provides a logbook of the spectroscopic observations. The visibility and integrated flux of the HeII 4686 Å emission line is given in Table 2. The values listed in Table 2 are averaged over all the spectra collected on the given observing night. The heliocentric radial velocity of the HeII 4686 Å emission

Table 3. Heliocentric radial velocity ($RV_{\odot}$) of HeII 4686 Å emission line measured on our individual spectra of KT Eri.

Date	HJD	$RV_{\odot}$ (km s^{-1})	Date	HJD	$RV_{\odot}$ (km s^{-1})
2010 Jan. 06	5203.264	–202	2010 Feb. 20	5248.332	–54
	5203.275	–230		5248.365	–84
2010 Jan. 18	5215.374	–101		5248.377	–103
	5215.382	–78		5248.389	–106
	5215.391	–70	2010 Mar. 16	5272.303	–71
2010 Jan. 24	5221.273	–89		5272.316	–59
	5221.283	–112	2013 Jan. 05	6298.389	–160
	5221.291	–97		6298.404	–186
	5221.391	–90		6298.418	–126
	5221.403	–84	2013 Jan. 06	6299.346	–245
	5221.415	–85		6299.368	–220
	5221.428	–81		6299.391	–251
2010 Jan. 28	5225.293	–86		6299.413	–237
	5225.305	–91	2013 Jan. 26	6319.319	–155
	5225.316	–64		6319.335	–177
	5225.327	–69		6319.351	–182
2010 Feb. 02	5230.292	–67	2013 Mar. 02	6354.253	–94
	5230.303	–58	2013 Mar. 04	6356.259	–224
	5230.315	–47	2013 Dec. 13	6640.355	–140
	5230.328	–39		6640.379	–164
2010 Feb. 06	5234.343	–240		6640.403	–75
	5234.354	–259	2014 Feb. 09	6698.265	–131
	5234.366	–249		6698.281	–130
2010 Feb. 13	5241.321	–38		6698.297	–134
	5241.343	–52		6698.330	–166
	5241.358	–49		6698.346	–162
2010 Feb. 13	5241.406	–74		6698.363	–116
	5241.442	–72	2014 Feb. 12	6701.243	–143
	5241.453	–137		6701.257	–201
	5241.465	–116		6701.271	–188
2010 Feb. 20	5248.258	–106		6701.287	–207
	5248.282	–79		6701.304	–185
	5248.309	–41		6701.320	–168
	5248.320	–68			

Notes. HJD = heliocentric JD - 2 450 000.

line, as measured on each individual collected spectrum, is listed in Table 3. The radial velocities are from Gaussian fits to the observed profiles. The observed HeII profile rapidly converged to a Gaussian-like profile shortly after the line appeared in emission. The profile at the earliest epochs was admittedly more structured than a simple Gaussian, but it was basically symmetric and therefore the fit with a Gaussian does not significantly affect the derived velocity, which is very similar to the velocity derived for the line photocenter. The typical measurement error for these Gaussian fits is 12 km s^{-1}. Any error in the wavelength calibration of the spectra is removed from the HeII radial velocities by subtracting from them the average velocity measured, on the sky background, for the two HgI city-light emission lines at 4358 and 5461 Å. These corrections are on the order of 10 km s^{-1} (corresponding to 7% of the velocity span of one pixel).

3. Spectral evolution and HeII lines

The spectral evolution of KT Eri during the 2009 outburst and the subsequent return to quiescence is presented in Fig. 1. The average pre-outburst mean B magnitude of KT Eri was around 15.4 mag (from Jurdana-Šepić et al. 2012, and the recalibration of their historical Harvard photographic data as performed by Munari & Dallaporta 2014). The average B-band magnitude of KT Eri during 2013 and 2014 is 15.3, which confirms that the object was back to quiescence level when we observed it in 2013 and 2014.

The spectrum for 2009 December 01 (day +17) is representative of those obtained immediately following the discovery of the nova (that happened +11 days past optical maximum). It is characterized by broad emission lines. The average FWHM of hydrogen Balmer and OI emission lines is 3200 km s^{-1}, while HeI lines are sharper with a FWHM of 950 km s^{-1}. The profile of the Balmer lines already shows hints of the two components – a broad pedestal and a superimposed sharper core – that will stand out clearly at later epochs. No HeII 4686 Å emission line was observed in our early spectra, including the Echelle for 2009 December 19, +35 day past maximum. Our next spectrum, for 2010 January 6, corresponding to day +53, shows a weak HeII in emission superimposed on the red wing of the strong NIII 4640 Å line. The exact day of the first appearance of HeII is day +48, as revealed by inspection of the compilation of spectra of KT Eri obtained with the Liverpool telescope + FRODOS spectrograph and summarized by Ribeiro (2011; one of these spectra is used to plot the left panel of Fig. 3 in place of our spectrum for the same date that was obtained at a lower resolution). The sample of spectra in Fig. 1 shows how the HeII line rapidly grows in equivalent width with the progress of the decline from maximum, and how HeII 4686 Å remains the strongest spectral feature during the subsequent phases of the outburst and the following return to quiescence.

The flux evolution of the HeII 4686 Å emission line is compared to the V-band light curve of KT Eri in Fig. 2. To transform the flux of HeII 4686 Å into a magnitude scale for an easier comparison with the nova evolution in the V-band, we computed its *magnitude* as

$$\mathrm{mag(HeII)} = -2.5 \times \log\left(\frac{\mathrm{flux}}{5.9 \times 10^{-8}}\right), \tag{1}$$

where the arbitrary constant 5.9×10^{-8} erg cm^{-2} s^{-1} is chosen so to cancel the shift in Fig. 2 between the V-band and the HeII light curves. Figures 2 aims to highlight two basic facts: (*a*) the HeII line appeared when the nova had declined by about 3.5/4.0 mag below maximum brightness, i.e., a characteristic time in the evolution of typical novae when the ejecta begin turning optically thin allowing direct vision of the central star (e.g., McLaughlin 1960; Munari 2012). The fact that the ejecta were becoming optically thin at that time is confirmed by the simultaneous huge increase in the soft component of the X-ray emission. The X-ray hardness ratio from Swift observations is plotted in the top panel of Fig. 2 that shows how the nova entered the so-called super-soft-source phase (SSS, Krautter 2008) around day +50, simultaneously with the appearance of HeII in the optical spectra; (*b*) after an initial surge in the intensity of the HeII line, by day +70 its integrated flux declined in pace with the decline of the nova in V-band. The proportionality of HeII flux and V-band brightness continued well into the quiescence phase.

The transition around day +70 in the flux evolution of HeII 4686 Å also marked a conspicuous change in its profile, which is well illustrated in Fig. 3. Day +70 also marks the time when the X-ray emission was reaching its maximum

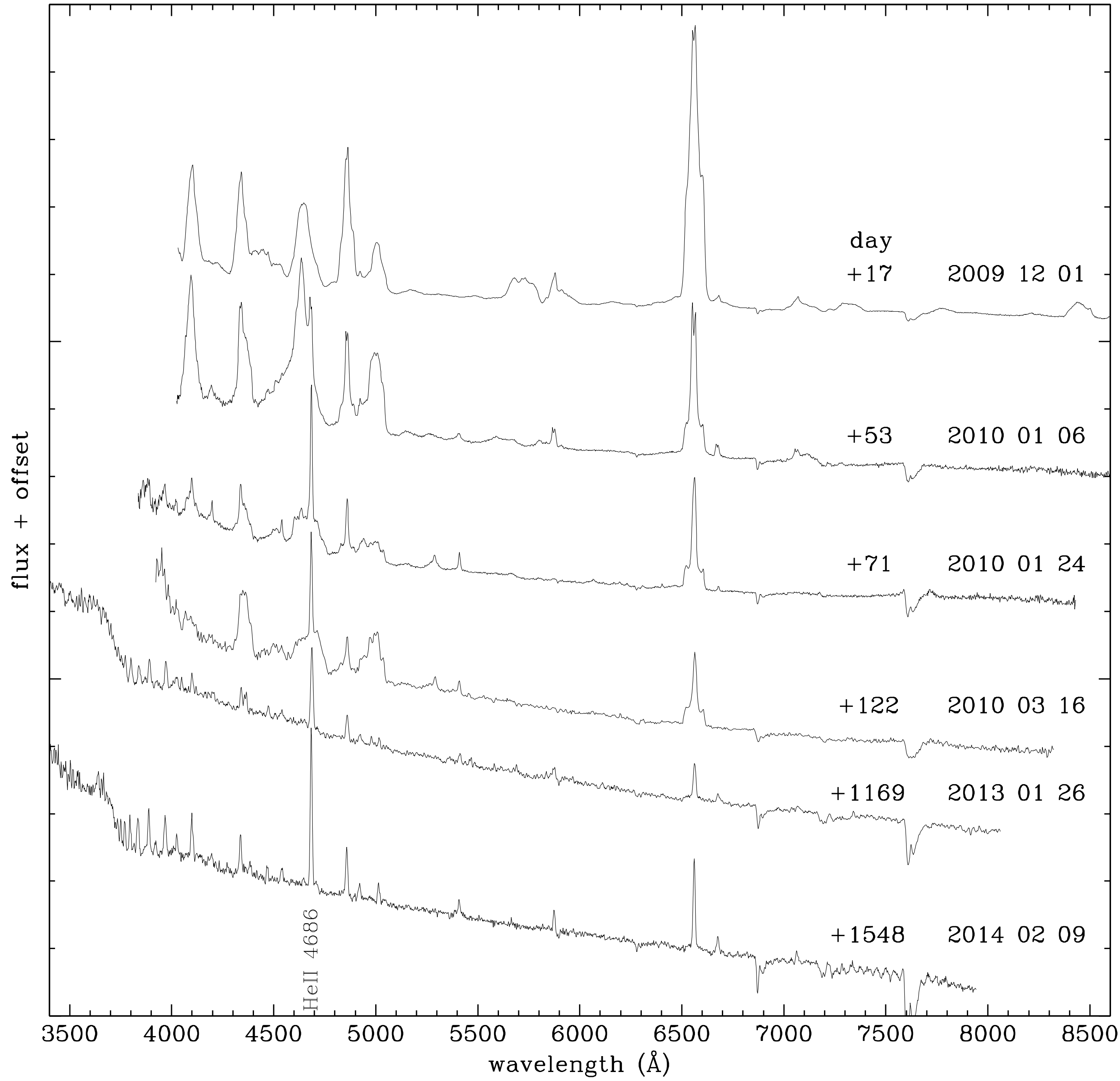

Fig. 1. Sample spectra from our monitoring to highlight the spectroscopic evolution of KT Eri during the 2009/10 nova outburst and the subsequent return to quiescence.

and initiating the SSS-plateau phase characterized by the lowest value of the hardness ratio (see top panel of Fig. 2).

Before day +70 (left panel in Fig. 3), HeII 4686 Å was similar to the narrow component of the Balmer lines. Both were double peaked and of similar width: 900 km s^{-1} for HeII 4686 Å and 1150 km s^{-1} for the Balmer lines. The width of the broad pedestal of the Balmer lines was 4500 km s^{-1}.

After day +70 (right panel in Fig. 3), the FWHM of HeII 4686 Å suddenly dropped by a factor of two, down to 460 km s^{-1}, while that of the Balmer lines remained around 1000 km s^{-1} for the narrow component and 4600 km s^{-1} for the pedestal.

Ribeiro et al. (2013) modeled the Hα profile during the early optically thick phase of KT Eri and found a good fit with dumbbell shaped expanding ejecta and no need for an equatorial ring. The dumbbell structure was characterized by a $1/r$ radial density profile, $V_{\rm exp} = 2800 \pm 200$ km s^{-1}, a major to minor axis ratio of 4:1, and an inclination angle of 58^{+6}_{-7} deg. The density profile $\rho \propto r^{-1}$ allowed Ribeiro et al. to fit the broad, square-like pedestal coming from the outer parts of the bipolar lobes and the narrow, double-peaked central component of the Hα profile coming from the slower and denser regions closer to the wrist, simultaneously.

When HeII 4686 Å was first weakly detected around day +48, and for the following period up to day +70, it came from the denser region of the ejecta closer to the wrist of the bipolar structure. This is the same region from where at earlier times the HeI lines came from. In fact, their FWHM (950 km s^{-1})

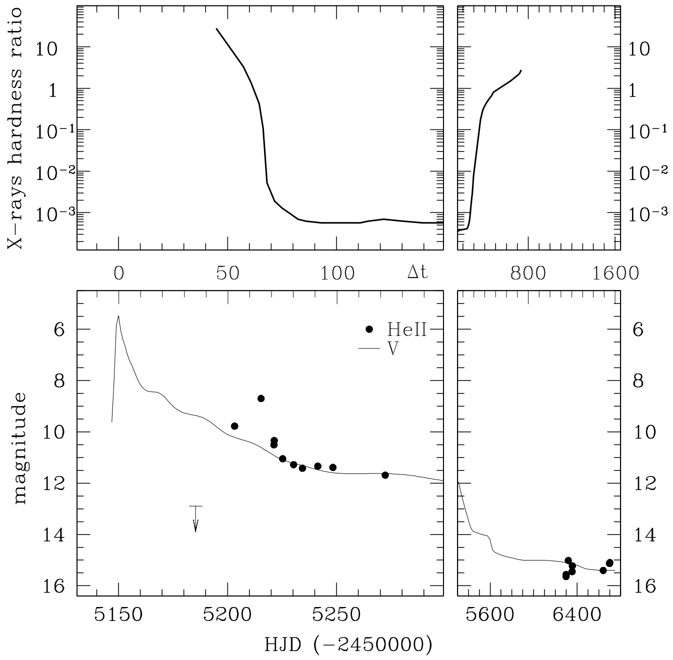

Fig. 2. Evolution of the integrated flux of HeII 4686 Å emission line of KT Eri compared to its *V*-band light curve (from Hounsell et al. 2010, AAVSO database, Munari & Dallaporta 2014, and unpublished recent data). To facilitate the comparison, the integrated line flux is transformed in magnitudes and offset by the quantity given in Eq. (1). The arrow marks the upper limit to HeII integrated flux on day +35 spectra. *Top panel*: the hardness ratio (defined as the ratio between the count rates in the 1–10 keV and 0.3–1 keV bands) of the Swift X-ray observations (adapted from public data available on the Swift web site).

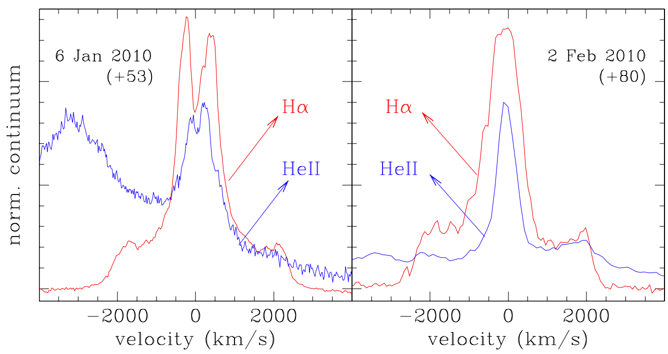

Fig. 3. Comparison between the line profiles of Hα and HeII 4686 Å for day +53 (ejecta still optically thick) and day +80 (ejecta now optically thin).

was very similar to that of HeII 4686 Å and the narrow component of the Balmer lines. The appearance of HeII 4686 Å (produced during the recombination of HeIII to HeII) was obviously related to the increase in temperature of the pseudo-photosphere contracting through the inner regions of the ejecta closer to the central star. As this contraction proceeded and the optical thickness of the ejecta continued to decline as a consequence of the ongoing expansion, a larger fraction of the inner ejecta were reached by hard ionizing photons and the intensity of HeII 4686 Å surged until a maximum was attained around day +65. The ionization of HeII into HeIII never reached the outer lobes of the ejecta, because the HeII lines never developed the broad pedestal displayed by the Balmer lines[2]. Following this maximum, the intensity of HeII 4686 Å began to decline in parallel to the other emission lines and to the underlying continuum.

Day +70 also marks the time when the continuum emission from the ejecta, now completely transparent, fell below that coming directly from the central star. As shown in Fig. 2, by day +70 (*a*) the X-ray emission entered the SSS plateau where it remained stable until day ∼250 which marks the end of the nuclear burning on the white dwarf, and (*b*) in parallel, the optical brightness of the KT Eri stopped declining because direct emission from the white dwarf and from the irradiated companion replaced that of fading ejecta; it rapidly dropped to the quiescence value only when the X-ray SSS phase ended. The broader HeII 4686 Å profile (FWHM 900 km s^{-1}) coming from the fading ejecta after day +70 is overwhelmed by the narrower profile originating directly from the central binary (FWHM 460 km s^{-1}). This will not happen for the Balmer lines until much later into the evolution, because (as shown by the quiescence spectrum from 2013 January 26, day +1169) the Balmer lines produced by the central star are quite weak and to emerge they need the emission from the ejecta to essentially vanish.

The sequences of spectra in Fig. 4 show how – past day +70 – the HeII 4686 Å emission originated directly from the central binary while the Balmer lines continue to come from the ejecta for a long time. Here the profiles of Hα, Hβ, and HeII 4686 Å from many different spectra obtained on 2010 February 2 and 6 (days +80 and +84) are compared. The profile and radial velocity of the Balmer lines, both their broad pedestal and their narrow component, do not change from one night to the other. The ∼200 km s^{-1} shift in radial velocity of HeII (from −53 to −249 km s^{-1}, see Table 3) is instead outstanding. Such continuous and large change in radial velocity of HeII 4686 Å cannot be easily understood in terms of ballistic expansion of nova ejecta, while they can be naturally accounted for by the continuously changing viewing geometry of the central binary and the instabilities inherent to mass transfer.

We have searched the epoch radial velocities in Table 3 looking for periodicities that could betray the orbital period of the nova. We have used the Fourier code implemented by Deeming (1975) for unequally spaced data. Extensive tests on the whole set of Table 3 data as well as on random selected subsamples failed to reveal any clear and strong periodicity. The situation is similar to that encountered in photometry (see Munari & Dallaporta 2014), where no other clear periodicity stands out in addition to the 752-day eclipse-like events that regularly marked the pre- and post-outburst optical photometry of KT Eri. The brightness of KT Eri varies similarly in all optical bands and by a large amplitude (on the order of one magnitude in *B*) with a timescale that is continously changing, in an apparently chaotic manner. The same seems to occur with the radial velocity of the HeII emission line, which is seen to change by large margins, but in an apparently chaotic pattern. This could be the result of the beating of several different true periodicities simultaneously present, but to disentangle them it will be necessary to accumulate many additional observations, possibly at a higher dispersion than the spectra used for the present study. Additional data, regularly spaced over many consecutive observing seasons, will be necessary to investigate the presence of the 752-day period among the spectral data.

[2] The apparent emission bump on the red side of the narrow HeII line in the left panel of Fig. 4 should be identified with other transitions within the blend, as, otherwise, we should observe a symmetric component on the blue side of HeII.

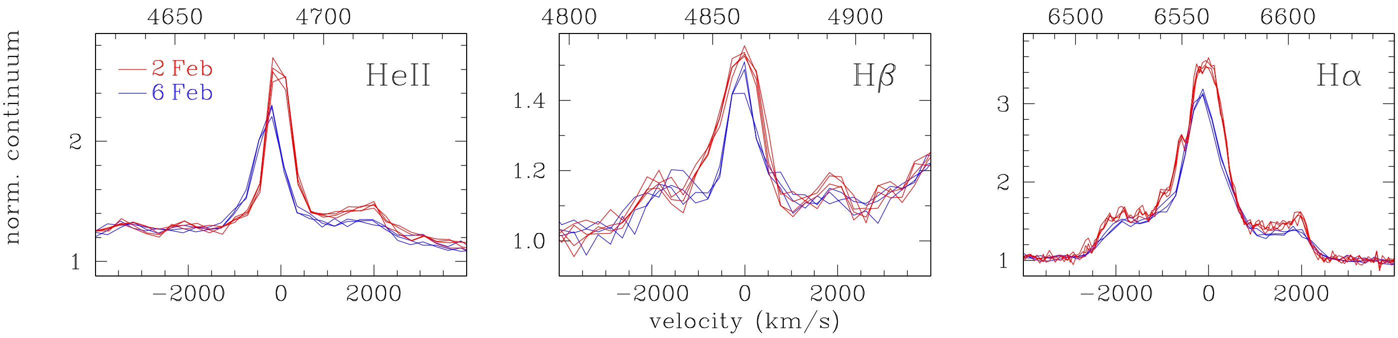

Fig. 4. Overplot of HeII 4686 Å, Hβ, and Hα lines from individual spectra obtained on 2010 February 2 and 6 (rebinned to the same, coarser wavelength scale of the later date). It is quite obvious how the large radial velocity change displayed by HeII between the two dates does not have a counterpart in the Balmer lines, neither the broad pedestal nor the narrower core.

Acknowledgements. We would like to thank A. Milani and V. Luppi of ANS Collaboration for their assistance with the observations obtained with the Varese 0.61 m telescope and Valerio A.R.M. Ribeiro for having promptly offered his higher quality spectrum for 6 Jan. 2010. EM thanks Steven N. Shore for valuable discussions.

References

Beardmore, A. P., Balman, S., Osborne, J. P., et al. 2010, ATel, 2423
Bode, M. F., Osborne, J. P., Page, K. L., et al. 2010, ATel, 2392
Deeming, T. J. 1975, Ap&SS, 36, 137
Hounsell, R., Bode, M. F., Hick, P. P., et al. 2010, ApJ, 724, 480
Hung, L. W., Chen, W. P., & Walter F. M. 2011, ASP Conf., 451, 271
Imamura, K., & Tanabe K. 2012, PASJ, 64, 120
Jurdana-Šepić, R., Ribeiro, V. A. R. M., Darnley, M. J., Munari, U., & Bode, M. F. 2012, A&A, 537, A34
Krautter, J. 2008, in Classical Novae 2nd edn., eds. M. F. Bode, & A. Evans (Cambridge Univ. Press), 232
Mason, E., Ederoclite, A., Williams, R. E., Della Valle, M., & Setiawan, J. 2012, A&A, 544, 149
Mason, E., & Walter, F. M. 2013, Stellae Novae: Future and past decades, ASP Conf. Ser., in press [arXiv:1303.2776]
McLaughlin, D. B. 1960, in Stellar atmospheres, ed. J. L. Greenstein (University of Chicago Press), 585
Munari, U. 2012, J. Am. Assoc. Var. Star Obs., 40, 582
Munari, U., & Dallaporta, S. 2014, New Astron., 27, 25
Munari, U., & Valisa, P. 2014, in Observing Techniques, Instrumentation and Science for Metre-class Telescopes (Workshop), eds. T. Pribulla, & V. Martin, CAOSP, in press
Munari, U., Ribeiro, V. A. R. M., Bode, M. F., & Saguner, T. 2011, MNRAS, 410, 525
Munari, U., Bacci, S., Baldinelli, L., et al. 2012, Baltic Astron., 21, 13
Ness, J.-U., Drake, J. J., Starrfield, S., et al. 2010, ATel, 2418
O'Brien, T. J., Muxlow, T. W. B., Stevens, J., et al. 2010, ATel, 2434
Gaposchkin, C. H. P. 1957, The galactic novae (Amsterdam: North-Holland Pub. Co.)
Ragan E., Brozek, T., Suchomska, K., et al. 2009, ATel, 2327
Raj, A., Banerjee, D. P. K., & Ashok, N. M. 2013, MNRAS, 433, 2657
Ribeiro, V. A. R. M., 2011, Ph.D. Thesis, Liverpool John Moores University
Ribeiro, V. A. R. M., Bode, M. F., Darnley, M. J., et al. 2013, MNRAS, 433, 1991
Rudy, R. J., Prater, T. R., Russell, R. W., Puetter, R. C., & Perry, R. B. 2009, Central Bureau Electronic Telegrams, 2055, 1
Walter, F. M., & Battisti, A. 2011, AAS, 217 338.11